

1 **Uptake of Neisserial autotransporter lipoprotein (NalP) promotes an**
2 **increase in human brain microvascular endothelial cell metabolic activity**

3

4 **Osman A. Dufailu, Jafar Mahdavi, Dlawer A. A. Ala’Aldeen¹, Karl G. Wooldridge and**
5 **Neil J. Oldfield***

6

7 School of Life Sciences, University of Nottingham, Nottingham, UK

8 ¹Present address: Middle East Research Institute, Dream City, Erbil, Kurdistan Region of Iraq

9

10 *For correspondence: Centre for Biomolecular Sciences, University of Nottingham,
11 University Park, Nottingham, NG7 2RD, UK. E: neil.oldfield@nottingham.ac.uk; T: (+44)
12 115 748 6122.

13 **Abstract**

14 *Neisseria meningitidis* is normally a human nasopharyngeal commensal but is also capable of
15 causing life-threatening sepsis and meningitis. *N. meningitidis* secretes several virulence-
16 associated proteins including Neisserial autotransporter lipoprotein (NalP), an immunogenic,
17 type Va autotransporter harboring an S8-family serine endopeptidase domain. NalP has been
18 previously characterized as a cell-surface maturation protease which processes other
19 virulence-associated meningococcal surface proteins, and as a factor contributing to the
20 survival of meningococci in human serum due to its ability to cleave complement factor C3.
21 Here, recombinant NalP (rNalP) fragments were purified and used to investigate the
22 interaction of NalP with host cells. Flow cytometry and confocal microscopy demonstrated
23 binding and uptake of rNalP into different human cell types. High-resolution microscopy
24 confirmed that internalized rNalP predominantly localized to the perinuclear region of cells.
25 Abolition of rNalP protease activity using site-directed mutagenesis did not influence uptake
26 or sub-cellular localization, but inactive rNalP (rNalP^{S426A}) was unable to induce an increase
27 in human brain microvascular endothelial cell metabolic activity provoked by proteolytically-
28 active rNalP. Our data suggests a more complex and multifaceted role for NalP in
29 meningococcal pathogenesis than was previously understood which includes novel intra-host
30 cell functions.

31

32 **Highlights:**

- 33 • Recombinant NalP is internalized by a variety of human cell types
- 34 • Internalized NalP is localized predominantly to the perinuclear region of cells
- 35 • Exposure to NalP provokes increases in cell metabolic activity
- 36 • Effects on cell metabolic activity are dependent on NalP proteolytic activity

37

38 Keywords: *Neisseria meningitidis*; autotransporter; NalP; cellular uptake; pathogenesis;
39 proteolysis

40

41 **1. Introduction**

42 *Neisseria meningitidis* is an encapsulated Gram-negative diplococcus commonly
43 carried in the human nasopharynx. Carriers usually remain asymptomatic, but rarely
44 meningococci can reach the bloodstream which may lead to sepsis, and the cerebral-spinal
45 fluid (CSF) which can result in meningitis [1]. *N. meningitidis* elaborates numerous virulence
46 factors that facilitate colonization and virulence [2]. One important class, which are also
47 found in many other Gram-negative bacteria, are the autotransporter (or type V-secreted)
48 proteins [3]. These comprise an N-terminal signal peptide and C-terminal β -domain, which
49 facilitate export of a central functional passenger domain across the Gram-negative inner and
50 outer membranes, respectively. Following export, the passenger domain may be cleaved and
51 released, either auto-catalytically or via a second protease, cleaved but remain non-covalently
52 bound to the translocator domain, or remain uncleaved and displayed at the cell surface [4].
53 Autotransporter passenger domains undertake a range of virulence-associated functions
54 including proteolytic, cytotoxic or adhesive activities [5].

55 The functional passenger domain of Neisserial autotransporter lipoprotein (NalP), also
56 termed autotransporter serine protease A (AspA), harbors an S8-family peptidase (subtilisin)
57 domain [6, 7]. Additionally, NalP expression is phase-variable via slipped strand mispairing,
58 a process mediated by a poly-cytosine tract within the protein-coding sequence [7, 8]. Auto-
59 catalytic proteolytic cleavage results in the release of a *ca.* 68-70 kDa passenger domain into
60 the external environment [6, 7]. However, a proportion of the cleaved passenger domains
61 remain, at least temporarily, anchored on the cell surface by an N-terminal lipid moiety [9].
62 This delayed or partial release facilitates the NalP-dependent proteolytic release of fragments

63 of other meningococcal surface proteins including: IgA1 protease; MspA (meningococcal
64 serine protease A); App (adhesion and penetration protein); LbpB (lactoferrin-binding
65 protein); and NHBA (Neisserial heparin binding antigen) [7, 10-14]. The consequences of the
66 NalP-mediated release of meningococcal surface protein fragments on pathogenesis are
67 beginning to be elucidated. For example, NalP-mediated release of NHBA abrogates
68 extracellular DNA-mediated biofilm formation [15]. Furthermore, the NHBA-derived C2
69 fragment released following cleavage by NalP alters endothelial integrity by producing
70 reactive oxygen species resulting in the internalization of the VE-cadherin adherens junction
71 protein [16].

72 In addition to meningococcal targets, NalP has also been shown to cleave the host
73 serum protein complement 3 (C3) [17]. NalP-mediated cleavage generates a functionally
74 inactive C3a-like molecule, with the corresponding C3b-like fragment being rapidly
75 inactivated by host serum factors resulting in the inhibition of C3b deposition on the bacterial
76 surface and enhanced meningococcal serum resistance [17]. We hypothesized that, in
77 addition to previously identified roles, NalP, like several other meningococcal autotransporter
78 proteases [18-20], may also interact with host cells. Here we show uptake of NalP into
79 various human cell types, and an increase in human brain microvascular endothelial cell
80 metabolic activity which is dependent on NalP proteolytic activity.

81

82 **2. Materials and Methods**

83 *2.1. Bacterial strains and culture conditions*

84 *Escherichia coli* strain JM109 (Promega) was used for expression of recombinant
85 His₆-tagged NalP passenger domain fragments. *E. coli* strain XL10-Gold (Agilent
86 Technologies) was used for mutagenic plasmid construction. Strains were cultured at 37°C in
87 Lysogeny broth (LB) or on LB agar supplemented with ampicillin (100 µg ml⁻¹). *N.*

88 *meningitidis* strain MC58 (ATCC® BAA335™) was cultured at 37°C, in an atmosphere of
89 air plus 5% CO₂, on Columbia agar with chocolated horse blood (Oxoid).

90

91 2.2. Construction of plasmids encoding recombinant NalP proteins

92 Primers NalPF1 (CGCGGATCCCTGCATACCGGAGACTTTCC) and NalPR1
93 (CGCGGATCCGCGGAGACTGTTGAAGATGCG) were used to amplify a fragment of *ca.* 2 kb
94 encoding amino acids ¹⁰¹L to ⁷⁸⁴A from *N. meningitidis* MC58 *nalP*. After digestion with
95 BamHI, the PCR product was ligated into BamHI-digested pQE30 to yield plasmid pOD1. A
96 single-nucleotide mutation (T to G) at nucleotide position 1276 of *nalP* was introduced into
97 pOD1 using the QuikChange Lightning site-directed mutagenesis kit (Agilent Technologies)
98 for expression of rNalP^{S426A}. The mutagenic reaction was undertaken following the
99 manufacturer's instructions and utilized primers t1276g S426A
100 (CCGATTCAAATTGCCGGAACAGCCTTTTCCGCACC) and t1276g_antisense
101 (GGTGCGGAAAAGGCTGTTCCGCAATTTGAATCGG) to yield pOD1^{S426A}.

102

103 2.3. Protein expression and purification

104 rNalP and rNalP^{S426A} were expressed in *E. coli* JM109 harboring pOD1, or
105 pOD1^{S426A}, respectively, and purified under non-denaturing conditions. Briefly, *E. coli*
106 JM109 strains were grown to OD₆₀₀ 0.5 before being induced with 1 mM IPTG and incubated
107 at 37°C for 3 h. Cells were harvested by centrifugation (4,200 × *g* for 10 min) and
108 resuspended in 30 ml lysis buffer (50 mM Na₂PO₄, 300 mM NaCl and 20 mM imidazole, pH
109 7.4) followed by sonication using a MSE SoniPrep 150 sonicator for 8 cycles (30s on, 30s
110 off) on ice. The cell lysate was centrifuged at 4,200 × *g* for 15 min and the cleared lysate
111 loaded onto a 1 ml Nickel-charged HisTrap FF column connected to a ÄKTAprime plus
112 liquid chromatography system (GE Healthcare Lifesciences) equilibrated with 10 column

113 volumes of wash buffer (50 mM Na₂PO₄, 300 mM NaCl and 40 mM imidazole, pH 7.4).
114 Proteins were eluted by step elution with appropriate buffer (50 mM Na₂PO₄, 300 mM NaCl
115 and 300 mM imidazole, pH 7.4). A HiTrap column pre-packed with five milliliters of
116 Sephadex G-25 Superfine (GE Healthcare Lifesciences) equilibrated with 5 column volumes
117 of phosphate buffered saline (PBS) was used for buffer exchange. His₆-tagged recombinant
118 *E. coli* trigger factor protein (rTF), encoded by the plasmid pCold TF (Takara Bio), was
119 purified as previously described [18]. Protein concentration was measured using the Pierce
120 BCA protein assay kit (Thermo Fisher Scientific) following endotoxin removal using Pierce
121 High Capacity Endotoxin removal spin columns (Thermo Fisher Scientific).

122

123 *2.4. SDS-PAGE and immunoblot analysis*

124 Proteins electrophoretically separated using polyacrylamide mini gels (Mini-Protean
125 III; Bio-Rad) were stained with SimplyBlue™ SafeStain (Thermo Fisher Scientific) for 1 h.
126 Alternatively proteins were transferred to nitrocellulose membranes and probed with rabbit
127 polyclonal anti-NalP [6] or mouse anti-pentahistidine antibody (Qiagen) diluted 1:5,000 or
128 1:2,000, respectively, in blocking buffer (5% [w/v] non-fat dry milk, 0.1% [v/v] Tween 20 in
129 1 × PBS) and incubated for 2 h. Following washing in PBS with 0.1% Tween 20 (PBST),
130 membranes were incubated for 2 h with goat anti-rabbit (or anti-mouse) IgG-alkaline
131 phosphatase conjugate (Sigma) at a dilution of 1:30,000 in blocking solution. After washing
132 with PBST, blots were developed using BCIP/NBT-Blue liquid substrate (Sigma).

133

134 *2.5. Cell culture*

135 All cells were maintained at 37°C in a humidified atmosphere of 5% CO₂. Cell culture
136 reagents were purchased from ScienCell unless otherwise stated. Human brain microvascular
137 endothelial cells (HBMECs-ATCC) were cultured on human fibronectin-coated flasks (BD

138 Biosciences) in basal endothelial cell medium, supplemented with 5% (v/v) heat-inactivated
139 fetal bovine albumin (FBS), 1 × endothelial cell growth supplement and 1% (v/v) antibiotic /
140 anti-mycotic solution. Dendritic cells were generated as previously [18], and subsequently
141 grown in RPMI (Sigma) supplemented with 10% FBS and 1% antibiotic / anti-mycotic.
142 Human brain (cerebral cortex) astrocytes (ScienCell) were cultured in astrocyte growth
143 medium supplemented with 5% FBS, 1 × astrocyte growth supplement and 1% antibiotic /
144 anti-mycotic. Hep-2 cells were cultured in DMEM (Sigma) supplemented with 10% FBS, 1 ×
145 non-essential amino acids (Sigma) and 1% antibiotic / anti-mycotic.

146

147 *2.6. Flow cytometry*

148 HBMECs were cultured on fibronectin-coated 24-well plates for 16 h from a seeding
149 density of 5×10^4 cells ml^{-1} . rNalP was atto488-labelled using the Lightning-Link
150 conjugation kit (Innova Biosciences) according to the manufacturer's instructions. Cells were
151 treated with atto488 alone, atto488-labelled rNalP or unlabeled rNalP (250 nM final
152 concentration dissolved in media) for 8 h. Cells were washed with PBS, fixed with 2%
153 paraformaldehyde for 10 min, and washed again with PBS before being detached using
154 trypsin-EDTA (Sigma). Harvested cells were washed twice with PBS and finally resuspended
155 in 500 μl of PBS. Samples were run on a FC500 flow cytometer (Beckman Coulter). 100,000
156 events were recorded, and acquired data was analyzed using Kaluza v1.3 software.

157

158 *2.7. Cell internalization assays*

159 Proteins were Cy5-labelled using the Lightning-Link conjugation kit (Innova
160 Biosciences) according to the manufacturer's instructions. Cells were seeded onto acid-
161 etched 12 mm glass coverslips (pre-coated with 0.1% human fibronectin for HBMECs) in 24-
162 well plates at a seeding density of 5×10^4 cells per well and incubated for 16 h. Cells were

163 treated with labelled rNaIP or rTF (250 nM final concentration dissolved in media) for 45
164 min, 2 h, 4 h or 8 h. After treatment, cells were washed thrice with PBS, fixed in 4%
165 paraformaldehyde for 10 min, and rinsed thrice in PBS. Cells were mounted using proLong
166 Gold anti-fade with DAPI (Life Technologies) to stain cell nuclei. Confocal imaging was
167 performed using a Zeiss LSM 700 confocal laser-scanning microscope using a Plan-
168 Apochromat 63×/1.40 Oil DIC M27 objective with ZEN 2009 operating software, and
169 equipped with lasers at 633 and 405 nm for excitation of Cy5 and DAPI, respectively. The
170 images collected in the two channels were later merged and analyzed using Zeiss LSM and
171 ImageJ software. Structured illumination microscopy (SIM) images were captured on a Zeiss
172 Elyra PS.1 microscope using an Objective alpha Plan-Apochromat 100×/1.46 Oil DIC M27
173 objective with ZEN 2012 acquisition and processing software. Samples were excited using
174 the 642 and 405 nm laser lines and fluorescence was detected using the LP 655 filter set. 3D
175 reconstruction was carried out using ZEN 2012 Black software. 30,000 images were
176 processed where single molecule events were identified with the peak intensity to noise value
177 set to ten.

178

179 *2.8. Human Complement 3 (C3) protein cleavage assay*

180 This was performed as previously described [17] with minor modifications. Briefly,
181 40 nM recombinant protein was mixed with 250 ng human complement 3 (C3; Sigma) in
182 PBS and incubated at 37°C with shaking for 16 h. C3 cleavage was determined by
183 immunoblot analysis using goat anti-human C3 antibody (diluted 1:5000; Sigma) and rabbit
184 anti-goat IgG alkaline phosphatase conjugate (diluted 1:30000; Sigma).

185

186 2.9. XTT assay

187 HBMECs were seeded in 96-well plates (1×10^4 cells well⁻¹) and grown overnight as
188 outlined in section 2.5. Cells were supplied with serum-free media and incubated at 37°C
189 with 5% CO₂ for 1 h before the addition of recombinant protein (40 nM final concentration)
190 and XTT detection solution (Cell Signaling Technologies). Cells were incubated for 37°C
191 with 5% CO₂ for 750 min and absorbance measurements (450 nm) taken using a Spark
192 microplate plate reader. Each test was performed in triplicate wells and on a least three
193 independent occasions. GraphPad Prism v7 was used to analyze the data using two-way
194 ANOVA and Tukey's multiple comparison test. A *p* value < 0.05 was considered statistically
195 significant.

196

197 2.10. Histone clipping

198 Recombinant core histones (New England Biolabs; 200 µg ml⁻¹ final concentration) and
199 purified recombinant protein (40nM final concentration) were mixed in a total volume of 40
200 µl PBS, and incubated at 37°C for 16 h. Reactions were stopped by the addition of 5 ×
201 sample buffer (0.62 M Tris-HCl [pH 6.8], 5% SDS, 25% glycerol, 12.5% β-mercaptoethanol,
202 0.25 M DTT, 0.002% bromophenol blue), followed by immediate boiling for 5 min. Aliquots
203 of cleavage products were subjected to SDS-PAGE, and gels stained with SimplyBlue™
204 SafeStain (Thermo Fisher Scientific).

205

206 **3. Results**

207 3.1. NalP is internalized by human cells

208 The passenger domain of the group B meningococcal strain MC58 NalP protein was
209 expressed in *E. coli* and purified under non-denaturing conditions to yield rNalP. Co-
210 incubation with human brain microvascular endothelial cells (HBMECs) followed by

211 examination by flow cytometry showing a clear shift in fluorescence signal in HBMECs
212 treated with fluorescently labelled rNalP compared with HBMECs treated with label alone or
213 with unlabeled rNalP, suggesting the direct interaction of rNalP with host cells (Fig. 1).
214 Confocal laser scanning microscopy was subsequently used to visualize rNalP following co-
215 incubation with HBMECs (Fig. 2). From 2 h co-incubation, internalized rNalP was primarily
216 apparent in crescent-like perinuclear accumulations (Fig. 2). In contrast, an unrelated His₆-
217 tagged recombinant protein (*E. coli* trigger factor; rTF), which was purified using the same
218 methodology as rNalP, was not internalized, demonstrating cellular specificity for rNalP
219 uptake (Fig. 2). Localization of internalized rNalP predominantly to the perinuclear region of
220 HBMECs was confirmed using high-resolution microscopy (Fig. S1). Examination by
221 confocal microscopy of other human cell types, including dendritic cells (DCs), epithelial
222 cells (Hep-2) and neural cells (astrocytes) showed that rNalP was also taken up by these cell
223 types and similarly localized to the cytoplasmic and/or perinuclear regions (Fig. S2).

224

225 *3.2. Uptake of proteolytically-active rNalP promotes an increase in HBMEC metabolic* 226 *activity*

227 Site-directed mutagenesis was used to replace the catalytic serine residue of rNalP
228 with alanine to generate rNalP^{S426A}. The abolition of proteolytic activity was confirmed by
229 the inability of rNalP^{S426A} to generate a *ca.* 100-kDa α -chain fragment following incubation
230 with the NalP target human complement factor C3 [17] (Fig. S3). Examination by confocal
231 microscopy showed no apparent differences in the localization of rNalP^{S426A} or rNalP in
232 HBMECs after co-incubation of cells with these proteins, showing that rNalP proteolytic
233 activity was not required for uptake or subsequent sub-cellular localization (Fig. 3).

234 To examine the cellular response to NalP, HBMECs were monitored post-exposure to
235 rNalP or rNalP^{S426A} using the XTT assay, which measures the ability of metabolically active

236 cells to reduce tetrazolium salt. From 270 min onwards, cells exposed to rNalP exhibited a
237 statistically significant increase in absorbance compared to untreated cells (Fig. 4). In
238 contrast, at no time point did HBMECs exposed to rNalP^{S426A} or rTF show significantly
239 different absorbance to untreated cells. As expected, cells exposed to the known apoptosis-
240 inducing agent staurosporine, which would be expected to reduce cellular metabolic activity,
241 had a significantly reduced absorbance evident from 120 min post-exposure. These data show
242 that rNalP can induce an increase in HBMEC metabolic activity and this effect is mediated
243 via the proteolytic activity of rNalP.

244 We previously showed that the meningococcal autotransporter proteins App and
245 MspA are capable of clipping the histone H3 [18]. To investigate potential cellular targets for
246 rNalP proteolytic activity, we examined the ability of rNalP and rNalP^{S426A} to cleave human
247 histones (H2A, H2B, H3.1 and H4) but the absence of rNalP-specific cleavage products
248 confirmed a lack of histone clipping activity (Fig. S4).

249

250 **4. Discussion**

251 NalP is an autotransporter protease which cleaves itself, and several other
252 meningococcal proteins, on the outer surface of the bacterium [7, 10-14]. Additionally, NalP
253 cleaves human C3, which contributes to meningococcal survival in human serum [17]. Here
254 we provide evidence that NalP is internalized by human cells and induces alterations in host
255 cell biology. This is reminiscent of findings from previous studies on the IgA1P, App and
256 MspA meningococcal serine protease autotransporters [18, 20, 21]. Following cellular uptake
257 and trafficking, IgA1P cleaves the p65/RelA component of NF- κ B in the nucleus, thus
258 silencing the expression of several NF- κ B-responsive genes, ultimately leading to sustained
259 activation of c-Jun N-terminal kinase and apoptosis [20]. App and MspA are also internalized
260 and induce apoptosis but, in contrast to IgA1P, MspA/App-mediated apoptosis occurs via

261 cleavage of histones [18]. The receptor of IgA1P uptake is unknown, whilst uptake of App
262 and MspA requires the cooperative activity of the mannose and transferrin receptors [18].
263 The wide range of cell types able to mediate NalP internalization (including immune,
264 epithelial, endothelial and neural cells) suggests shared receptor and internalization
265 machineries, but this will require further experimentation. Additional work is also required to
266 define the region(s) of NalP which are involved, although our data shows that uptake is not
267 dependent on the proteolytic ability of NalP.

268 The contribution of NalP to pathogenesis remains incompletely understood, in part
269 because of its low abundance in culture supernatants, which has impeded the purification of
270 experimentally useful amounts of active NalP directly from meningococcal cultures.
271 Consequently, previous studies have utilized *E. coli*-derived recombinant NalP fragments
272 purified under denaturing conditions (*i.e.* non-proteolytically active) or concentrated
273 secretome preparations derived from *N. meningitidis*, which although containing active NalP,
274 lacked purity. Furthermore, wild-type and *nalP* mutant-derived secretomes are difficult to
275 compare directly given the complex alterations in secreted protein profile that are NalP-
276 expression dependent [7, 9-14, 20]. The ability of our rNalP preparation, which was purified
277 under non-denaturing conditions, to cleave human C3, confirmed the findings of Del Tordello
278 *et al.*, [17], demonstrated that the recombinant protein was catalytically active, and
279 importantly provided the opportunity to specifically address the influence of NalP and its
280 proteolytic activity in inducing changes in host cell biology. This was determined using the
281 XTT assay – an assay based on the ability of dehydrogenase enzymes produced by
282 metabolically-active cells to reduce XTT to an orange formazan dye [22]. Significant
283 alterations in the ability to reduce XTT usually result from changes in cell viability following
284 exposure to a treatment. Additional work is required to investigate if the positive effect
285 mediated by rNalP occurs in other human cell types, whether it results from increased

286 proliferation, and to define the mechanism by which the effect occurs. Our data confirm,
287 however, that the observed effect is not mediated via NalP-mediated histone clipping.

288 In summary, the use of proteolytically-active recombinant NalP has generated new
289 insights into the multifaceted role of NalP in the complex interaction between the
290 meningococcus and its obligate host by revealing that NalP is internalized by host cells and
291 that NalP proteolytic activity results in an increase in cell metabolic activity.

292

293 **Funding**

294 This work was financially supported by the Ghana Education Trust Fund (GETFund).

295

296 **Acknowledgements**

297 We thank Dr A. Aslam (University of Nottingham, UK) for technical assistance during the
298 purification of recombinant proteins. Microscopy was carried out in the University of
299 Nottingham, School of Life Sciences Imaging Unit (SLIM).

300

301 **Conflicts of interest**

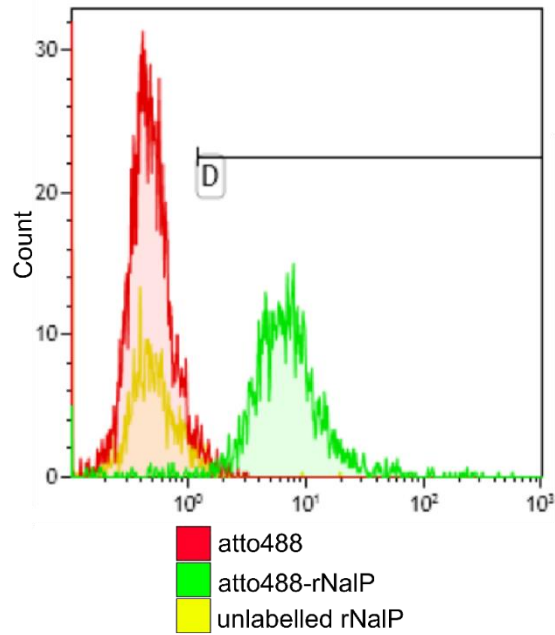
302 The authors declare that there are no conflicts of interest.

303 **References**

- 304 1. **Stephens DS.** Biology and pathogenesis of the evolutionarily successful, obligate
305 human bacterium *Neisseria meningitidis*. *Vaccine* 2009;27(Suppl 2):B71-77.
- 306 2. **Virji M.** Pathogenic neisseriae: surface modulation, pathogenesis and infection control.
307 *Nature* 2009;7:274-286.
- 308 3. **Henderson IR, Navarro-Garcia F, Desvaux M, Fernandez RC, Ala'Aldeen DAA.**
309 Type V protein secretion pathway: the autotransporter story. *Microbiol Mol Biol Rev*
310 2004;68(4):692-744.
- 311 4. **Leyton DL, Rossiter AE, Henderson IR.** From self sufficiency to dependence:
312 mechanisms and factors important for autotransporter biogenesis. *Nat Rev Microbiol*
313 2012;10:213-225.
- 314 5. **Benz I, Schmidt MA.** Structures and functions of autotransporter proteins in microbial
315 pathogens. *Int J Med Microbiol* 2011;301(6):461-468.
- 316 6. **Turner DPJ, Wooldridge KG, Ala'Aldeen DAA.** Autotransported serine protease A
317 of *Neisseria meningitidis*: an immunogenic, surface-exposed outer membrane, and secreted
318 protein. *Infect Immun* 2002;70(8):4447-4461.
- 319 7. **van Ulsen P, van Alphen L, ten Hove J, Fransen F, van der Ley P et al.** A Neisserial
320 autotransporter NalP modulating the processing of other autotransporters. *Mol Microbiol*
321 2003;50(3):1017-1030.
- 322 8. **Oldfield NJ, Matar S, Bidmos FA, Alamro M, Neal KR et al.** Prevalence and phase
323 variable expression status of two autotransporters, NalP and MspA, in carriage and disease
324 isolates of *Neisseria meningitidis*. *PLoS One* 2013;8(7):e69746.
- 325 9. **Roussel-Jazédé V, Grijpstra J, van Dam V, Tommassen J, van Ulsen P.** Lipidation
326 of the autotransporter NalP of *Neisseria meningitidis* is required for its function in the release
327 of cell-surface-exposed proteins. *Microbiology* 2013;159(Pt 2):286-295.

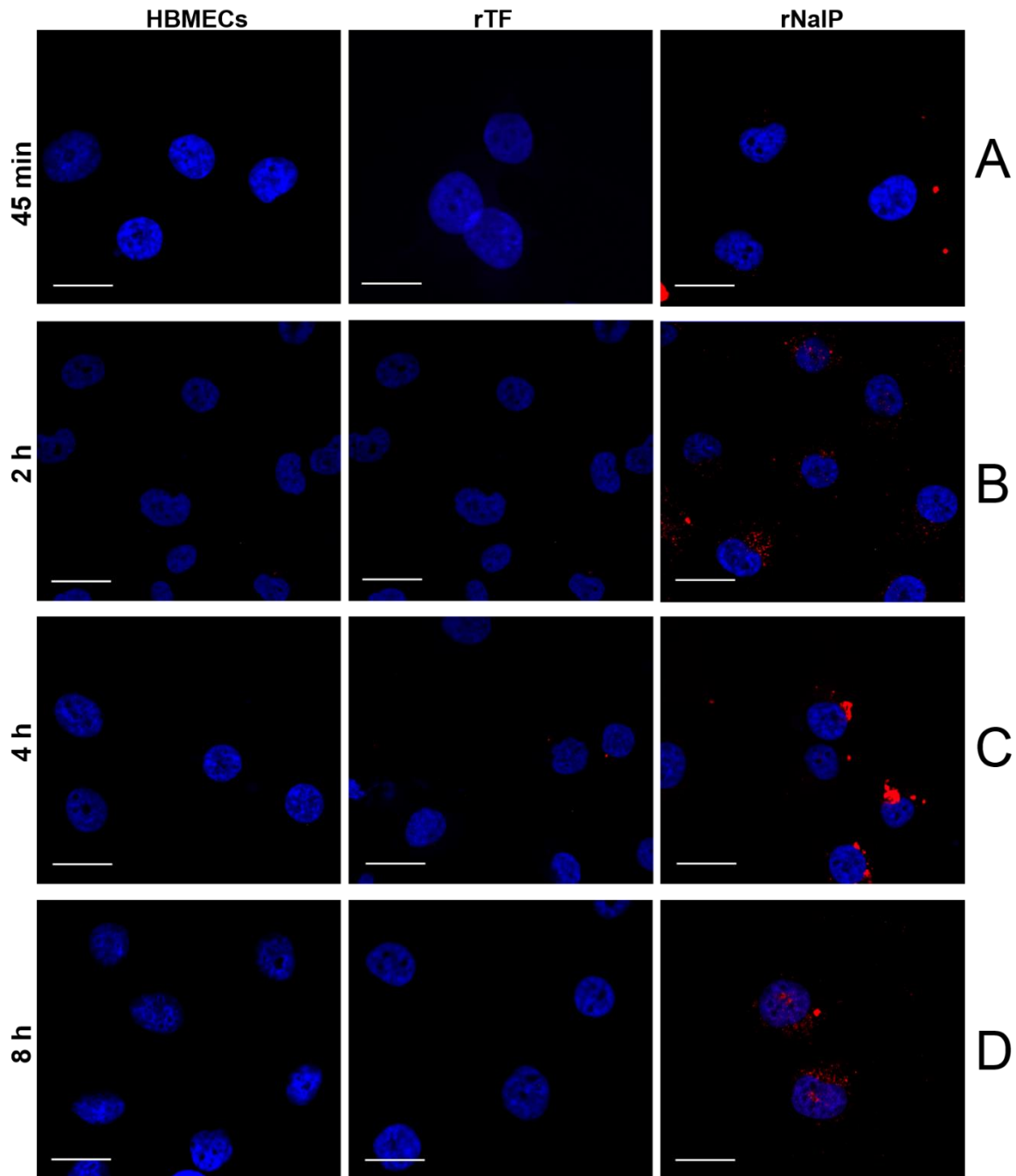
- 328 10. **Serruto D, Adu-Bobie J, Scarselli M, Veggi D, Pizza M et al.** *Neisseria meningitidis*
329 App, a new adhesin with autocatalytic serine protease activity. *Mol Microbiol* 2003;48(2):323-
330 334.
- 331 11. **Roussel-Jazédé V, Jongerius I, Bos MP, Tommassen J, van Ulsen P.** NalP-mediated
332 proteolytic release of lactoferrin-binding protein B from the meningococcal cell surface. *Infect*
333 *Immun* 2010;78(7):3083-3089.
- 334 12. **Serruto D, Spadafina T, Ciucchi L, Lewis LA, Ram S et al.** *Neisseria meningitidis*
335 GNA2132, a heparin-binding protein that induces protective immunity in humans. *PNAS*
336 2010;107(8):3770-3775.
- 337 13. **van Ulsen P, Adler B, Fassler P, Gilbert M, van Schilfgaarde M et al.** A novel phase-
338 variable autotransporter serine protease, AusI, of *Neisseria meningitidis*. *Microbes Infect*
339 2006;8(8):2088-2097.
- 340 14. **Turner DPJ, Marietou AG, Johnston L, Ho KK, Rogers AJ et al.** Characterization
341 of MspA, an immunogenic autotransporter protein that mediates adhesion to epithelial and
342 endothelial cells in *Neisseria meningitidis*. *Infect Immun* 2006;74(5):2957-2964.
- 343 15. **Arenas J, Nijland R, Rodriguez F, Bosma T, Tommassen J.** Involvement of three
344 meningococcal surface-exposed proteins, the heparin-binding protein NhbA, the α -peptide of
345 IgA protease, and the autotransporter protease NalP, in initiation of biofilm formation. *Mol*
346 *Microbiol* 2013;87:254-268.
- 347 16. **Casellato A, Rossi Paccani S, Barrile R, Bossi F, Ciucchi L et al.** The C2 fragment
348 from *Neisseria meningitidis* antigen NHBA increases endothelial permeability by destabilizing
349 adherens junctions. *Cell Microbiol* 2014;16(6):925-937.
- 350 17. **Del Tordello E, Vacca I, Ram S, Rappuoli R, Serruto D.** *Neisseria meningitidis* NalP
351 cleaves human complement C3, facilitating degradation of C3b and survival in human serum.
352 *PNAS* 2014;111(1):427-432.

- 353 18. **Khairalla AS, Omer SA, Mahdavi J, Aslam A, Dufailu OA et al.** Nuclear trafficking,
354 histone cleavage and induction of apoptosis by the meningococcal App and MspA
355 autotransporters. *Cell Microbiol* 2015;17(7):1008-1020.
- 356 19. **Lin L, Ayala P, Larson J, Mulks M, Fukuda M et al.** The Neisseria type 2 IgA1
357 protease cleaves LAMP1 and promotes survival of bacteria within epithelial cells. *Mol*
358 *Microbiol* 1997;24(5):1083-1094.
- 359 20. **Besbes A, Le Goff S, Antunes A, Terrade A, Hong E et al.** Hyperinvasive
360 meningococci induce intra-nuclear cleavage of the NF-kappaB protein p65/RelA by
361 meningococcal IgA protease. *PLoS Pathog* 2015;11(8):e1005078.
- 362 21. **Pohlner J, Langenberg U, Wölk U, Beck SC, Meyer TF.** Uptake and nuclear
363 transport of Neisseria IgA1 protease-associated α -proteins in human cells. *Mol Microbiol*
364 1995;17(6):1073-1083.
- 365 22. **Scudiero DA, Shoemaker RH, Paull KD, Monks A, Tierney S et al.** Evaluation of a
366 soluble tetrazolium/formazan assay for cell growth and drug sensitivity in culture using human
367 and other tumor cell lines. *Cancer Res* 1988;48(17):4827-4833.



368

369 **Fig. 1. Flow cytometric analysis showing the binding of rNalP to human brain**
370 **microvascular endothelial cells (HBMECs).** HBMECs treated with atto488 alone (red)
371 were compared with HBMECs treated with atto488-rNalP (green) and unlabeled rNalP
372 (yellow). Data was acquired on a Beckman Coulter FC500 flow cytometer and is displayed as
373 a histogram. The histogram area in D represents the population of fluorescently labelled
374 HBMECs.



375

376

Fig. 2. Cellular uptake of rNalP into human brain microvascular endothelial cells

377

(HBMECs). HBMECs were left untreated or co-incubated with Cy5-labelled rTF or rNalP

378

for 45 min (A), 2 h (B), 4 h (C) or 8 h (D). Cell nuclei were stained with DAPI. Cells were

379

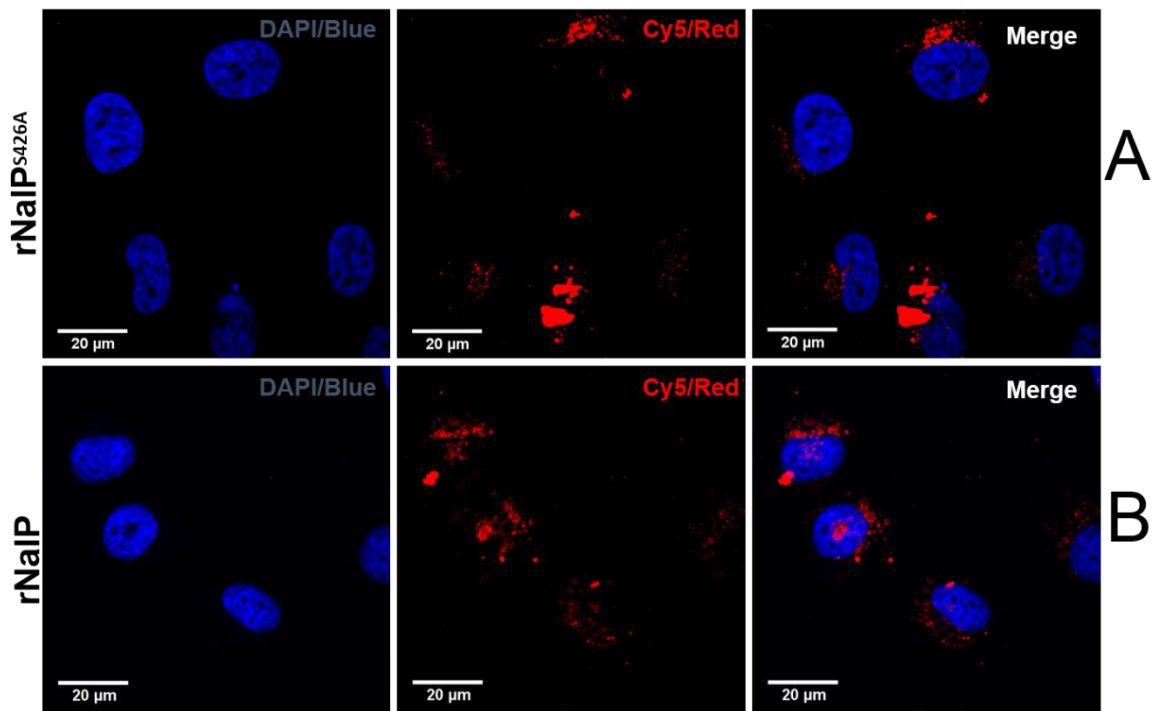
washed and fixed before analysis by confocal laser microscopy. All images were scanned at a

380

resolution of 1024×1024 pixels, using the same laser and gains settings. The cells are

381

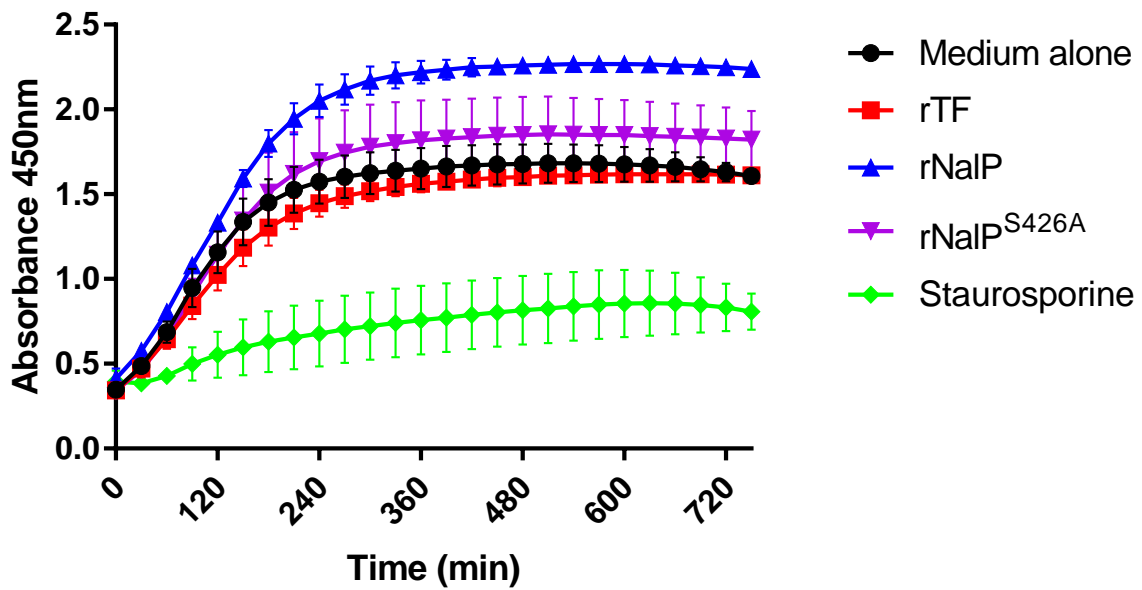
representative of cells observed from three independent experiments. Scale bars = $20 \mu\text{m}$.



383

384 **Fig. 3. rNaIP proteolytic activity is not required for cellular uptake and perinuclear**
 385 **localization by HBMECs.** HBMECs were treated with Cy5-labelled rNaIP^{S426A} (A) or rNaIP
 386 (B) for 8 h. Cell nuclei were stained with DAPI, washed and fixed before scanning using
 387 confocal laser microscope. All images were scanned at a resolution of 1024×1024 pixels,
 388 using the same laser and gains settings. The cells are representative of cells observed from
 389 multiple experiments. Scale bars = 20 μm .

390



391

392 **Fig. 4. Exposure of HBMECs to rNaIP induces an increase in cell metabolic activity.**

393 HBMECs were treated with medium alone, rTF, rNaIP, rNaIP^{S426A} or staurosporine in
394 triplicate. Cell metabolic activity was assessed using the XTT assay kit via absorbance
395 readings at 450 nm over 750 min. Values shown are the mean \pm SE from three independent
396 experiments and were analyzed by two-way ANOVA and Tukey's multiple comparison test.
397 Significant increases in absorbance were induced by rNaIP ($p < 0.05$ from 270 min; $p < 0.005$
398 from 600 min). rNaIP^{S426A} and rTF induced no significant difference compared to media
399 alone at any time point, whilst staurosporine induced a significant reduction in absorbance
400 compared to treatment with media alone ($p < 0.01$ from 120 min; $p < 0.001$ from 150 min;
401 $p < 0.0001$ from 180 min).